NMDA Receptor-Dependent Ocular Dominance Plasticity in Adult Visual Cortex

Nathaniel B. Sawtell, Mikhail Y. Frenkel,
Benjamin D. Philpot, Kazu Nakazawa,
Susumu Tonegawa, and Mark F. Bear*
Howard Hughes Medical Institute
The Picower Center for Learning & Memory
Department of Brain & Cognitive Sciences
Massachusetts Institute of Technology
Cambridge, Massachusetts 02139

Summary

The binocular region of mouse visual cortex is strongly dominated by inputs from the contralateral eye. Here we show in adult mice that depriving the dominant contralateral eye of vision leads to a persistent, NMDA receptor-dependent enhancement of the weak ipsilateral-eye inputs. These data provide in vivo evidence for metaplasticity as a mechanism for binocular competition and demonstrate that an ocular dominance shift can occur solely by the mechanisms of response enhancement. They also show that adult mouse visual cortex has a far greater potential for experience-dependent plasticity than previously appreciated. These insights may force a revision in how data on ocular dominance plasticity in mutant mice have been interpreted.

Introduction

The responses of neocortical neurons can be persistently modified by alterations in sensory experience. Such modifications reflect changes in synaptic transmission that shape cortical circuits and store information. Among the most extensively studied and well-characterized forms of experience-dependent plasticity are the effects of early visual deprivation on ocular dominance (OD) in the developing primary visual cortex. The pioneering studies of Wiesel and Hubel first demonstrated in kittens that if one eye is deprived of vision during the second postnatal month, a dramatic shift in cortical OD may occur, such that the majority of neurons in the primary visual cortex (area 17) no longer respond to visual input from the deprived eye (Wiesel and Hubel, 1963). Recently, the advent of transgenic and gene-targeting technologies has encouraged the use of mice to study the molecular requirements of OD plasticity (Gordon, 1997; Gordon and Stryker, 1996), as well as the mechanisms that limit visual cortical plasticity to an early critical period (Fagiolini and Hensch, 2000; Hanover et al., 1999; Hensch et al., 1998; Huang et al., 1999). A central premise underlying these investigations is that the phenomenon of OD plasticity in the mouse closely resembles that which has been characterized previously in cats and primates.

A standard method to study effects of monocular deprivation (MD) in rodents is to record visually evoked potentials (VEPs) from the surface of the binocular zone

*Correspondence: mbear@mit.edu

of primary visual cortex in anesthetized animals. VEPs reflect population synaptic currents, and the ratio of VEP amplitudes evoked by alternating patterned visual stimulation of the two eyes provides a reliable index of OD (Porciatti et al., 1999). Recordings from normally reared mice show a strong contralateral-eye dominance, and this can be shifted by temporarily suturing the contralateral eyelid during a critical period (Huang et al., 1999). VEP measurements of the initial contralateral bias and effects of subsequent MD are in excellent agreement with the OD distributions of single units recorded in the mouse under conditions of similar visual experience (Drager, 1978; Gordon and Stryker, 1996; Hanover et al., 1999). VEPs have the advantages that they are less subject to sampling bias, the data are quantitative (absolute levels of response, in addition to ratios), and they can be recorded chronically to yield information about the kinetics of synaptic plasticity (as shown below). In this study, we used VEP recordings in wild-type and mutant mice to demonstrate a novel form of OD plasticity and to determine the mechanism.

Results

Effects of Monocular Deprivation Persist beyond the Critical Period

The initial aim of our study was to confirm the developmental changes in OD plasticity in C57BL/6 mice in anticipation of studying various mutants. At all ages examined, we found that area 17 of nondeprived anesthetized mice was dominated by the contralateral eye, such that contralateral-eye VEP amplitudes were on average three times larger than the ipsilateral-eye (Figure 1B). MD of the contralateral eye for 3 days starting at postnatal day (P) 23 strongly shifted ocular dominance (Figure 1B), and this response to deprivation declined sharply with age (P36 contralateral-eye VEP/ ipsilateral-eye VEP (C/I) = 2.86 ± 0.67; n = 3; P60–P90 C/I = 3.15 ± 0.93; n = 4). These results are in agreement with previous reports characterizing the critical period for brief MD with single-unit recordings (Gordon and Stryker, 1996) and VEPs (Huang et al., 1999).

Unexpectedly, however, we found that the ocular dominance shift caused by a slightly longer period of deprivation—5 days—diminished only moderately with age. Significant effects of 5 day MD were observed in animals as old as P90 (P46–P52, C/I = 1.99 ± 0.41, n = 10, different from age-matched nondeprived controls at p < 0.02, t test; P60–P90, C/I = 2.15 ± 0.28, n = 7, p < 0.05). In a follow-up study, we specifically compared the effects of 3 versus 5 days of MD in adult mice (P60–P90; Figure 1C). In agreement with our initial finding, 5 but not 3 days of deprivation resulted in a C/I VEP ratio significantly different from nondeprived (ND) mice (p < 0.002, Fisher's PLSD).

These results presented a paradox since it has been established in other species that deprivation-induced synaptic depression is greatly attenuated or absent after adolescence (Heynen et al., 2003; Kossut and Singer,
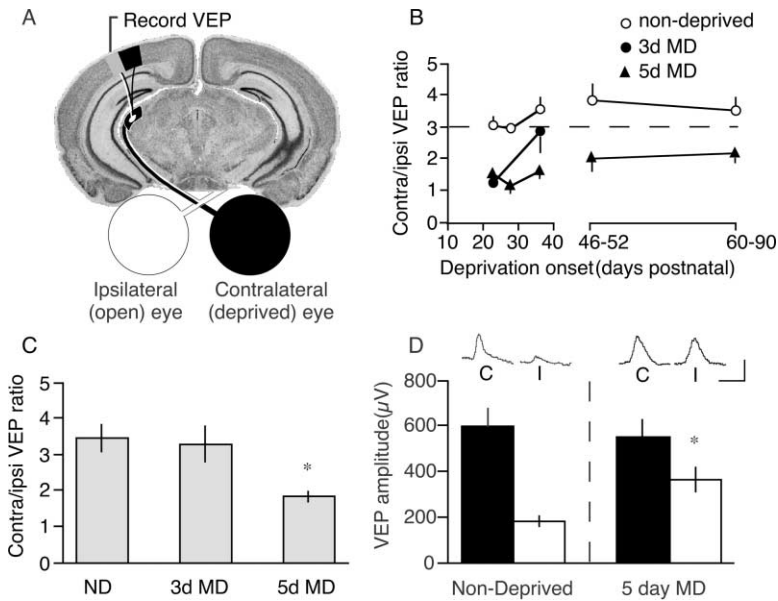
Figure 1. Effects of 3 but Not 5 Day MD Are Restricted to an Early Postnatal Critical Period in the Anesthetized Mouse

(A) Schematic of the mouse visual pathway and position of the recording electrode. VEPs were elicited by a pattern-reversing sinusoidal grating and recorded at the dural surface of the binocular zone (shaded).

(B) Contra/ipsi (C/I) VEP ratios were measured across a range of postnatal ages in nondeprived (open circles), 3 day MD (filled circles), and 5 day MD (filled triangles) mice. C/I VEP ratios were calculated by dividing the average VEP amplitude elicited by contralateral-eye stimulation by the average VEP amplitude elicited by ipsilateral-eye stimulation. Data for each group are presented as mean C/I ratio ± SEM.

(C) Differential effects of 3 and 5 day MD in adult mice (P60–90) were confirmed in an additional group of animals. Nondeprived (ND) C/I = 3.45 ± 0.37, n = 8; 3 day MD C/I = 3.29 ± 0.47, n = 10; 5 day MD C/I = 1.84 ± 0.14, n = 7.

(D) Contralateral (filled bars) and ipsilateral (open bars) VEP amplitudes in mice aged beyond the critical period (P36–P60, animals from [B] and [C]). Typical contralateral (C) and ipsilateral (I) VEP waveforms are displayed from nondeprived (left) and 5 day MD (right) mice. Scale bar, 0.4mV, 0.2 s.

1991; Mioche and Singer, 1989; Mitzdorf and Singer, 1980). Post hoc analysis of VEP amplitudes suggested an interesting resolution. The shift in C/I ratios observed in animals older than P36 appeared to result from a significant *increase* in open-eye VEP amplitudes (nondeprived 182.77μV ± 24.1μV, n = 27; 5 day MD 372.14μV ± 53.44μV, n = 24, p < 0.002; Figure 1D), with only a slight (nonsignificant) reduction in deprived-eye VEPs (nondeprived 598.57μV ± 74.6μV, n = 27; 5 day MD 558.68μV ± 75.7μV, n = 24, p > 0.5; Figure 1D). To pursue this intriguing finding, we developed a chronic preparation in which VEPs could be recorded in awake, head-restrained mice before, during, and after manipulations of visual experience.

VEP Recordings in Visual Cortex of Awake Mice

Because chronic VEP recordings had not been attempted previously in mice, we first analyzed the laminar pattern of cortical activation in awake animals. A recording electrode was tracked ventrally through area 17 in 100 μm steps from the dural surface to below the white matter (>1.3 mm). After each 100 μm advancement of the electrode, at least 150 VEPs were collected and averaged for each viewing condition. A representative example of the cortical VEP depth profile is presented in the left column of Figure 2. VEP waveforms recorded through the depth of the cortex were typically composed of an initial negativity followed by a more variable positivity. These components correspond roughly with N80 and P125 described in the primate (Schroeder et al., 1991). The VEP with the maximum negativity and shortest latency was recorded at a depth corresponding to layer IV (~400 μm). As expected, stimulation of the contralateral eye evoked stronger responses than ipsilateral-eye stimulation (Figures 2B and 2C). However, we consistently found in this study that the initial contralateral eye bias in the awake preparation (C/I = 2.3 ± 0.3)

was less pronounced than that observed in the anesthetized animals.

A one-dimensional current source density (CSD) analysis (Mitzdorf, 1985) was performed to determine the transmembrane currents responsible for the VEP waveforms at different depths (Figure 2, middle and right columns). A short latency current sink was observed in layer IV/deep III, with corresponding sources located in adjacent extragranular layers. This response was followed by sinks in supra- and infragranular layers, with the latency increasing with distance from layer IV. Although slight variations were observed between preparations (n = 5), the laminar pattern and temporal order of transmembrane currents were consistent across animals. Based on these data, we chose a recording depth of 400 μm for our chronic recording experiments and used the difference between the negative and positive peaks as our routine measure of VEP amplitude.

Real-Time Recording of Ocular Dominance Plasticity in Adult Mice

To investigate the consequences of adult MD, animals were implanted with chronic recording electrodes in area 17 of both hemispheres (Figures 3A and 3B). After a stable baseline was established, one eye was sutured shut. The median age at MD onset was P78 (range: P72–P90). VEPs were then recorded in response to open-eye stimulation for a period of 10–20 days, after which the deprived eye was reopened. Data from a representative animal are displayed in Figures 3A and 3B. In agreement with our previous findings in acute preparations, VEP amplitudes recorded in visual cortex ipsilateral to the open eye (IOE) increased substantially from days 3 to 5 of MD (Figure 3A). This increase remained after reopening the deprived eye such that cortical responses to contralateral- and ipsilateral-eye stimulation were nearly equal. For analysis of group data, VEP ampli-

A Binocular

FP · CSD · CSD Image

0.01 mVmm⁻² | 50 ms

Σ Source / Sink

Sink | Source

B Contralateral

FP · CSD · CSD Image

Σ

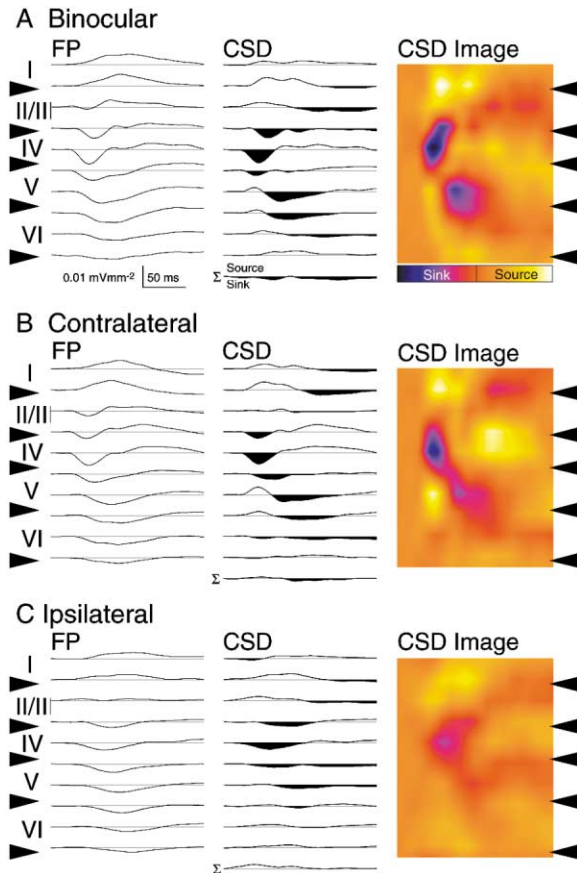## C Ipsilateral

FP · CSD · CSD Image

Σ

Figure 2. Laminar Activation Profiles Produced by Pattern Visual Stimulation in the Awake Mouse

The left column in (A), (B), and (C) shows field potentials (FPs) recorded at different cortical depths in response to binocular, contralateral-, or ipsilateral-eye stimulation, respectively. Cortical layers and boundaries (arrowheads) are indicated at the left of each panel. The middle column of (A), (B), and (C) presents CSD profiles obtained from the FPs using a spatial differentiation grid of 200 μM. Current sinks are downward and shaded, and current sources are upward going. The bottom trace (Σ) is summation of all CSD traces across depth. The right column of (A), (B), and (C) presents color image plots of CSD data. Cool colors (purple and blue) represent current sinks, and hot colors (yellow and white) represent current sources; orange is approximately zero. The color scale has been interpolated across depth (Aizenman et al., 1996).

tudes for each animal were normalized to a period of stable baseline recording, collapsed into 3 day bins, and averaged across animals. Significant increases in VEP amplitudes recorded ipsilateral to the open eye were observed following MD [Figure 3C; repeated measures ANOVA; $F(6,42) = 22.08$; $p < 0.001$]. The increase in open-eye VEP amplitude in this hemisphere was 173% $\pm$ 13% of baseline after 9–12 days of MD (n = 8). Interestingly, however, no significant changes in open-eye VEP amplitudes were observed in the visual cortex contralateral to this eye (n = 6; Figure 3D). Ipsilateral-eye VEPs also did not potentiate in response to 6 days of BD (post/pre = 0.82 $\pm$ 0.17; n = 4), showing that the response enhancement after MD is experience dependent.

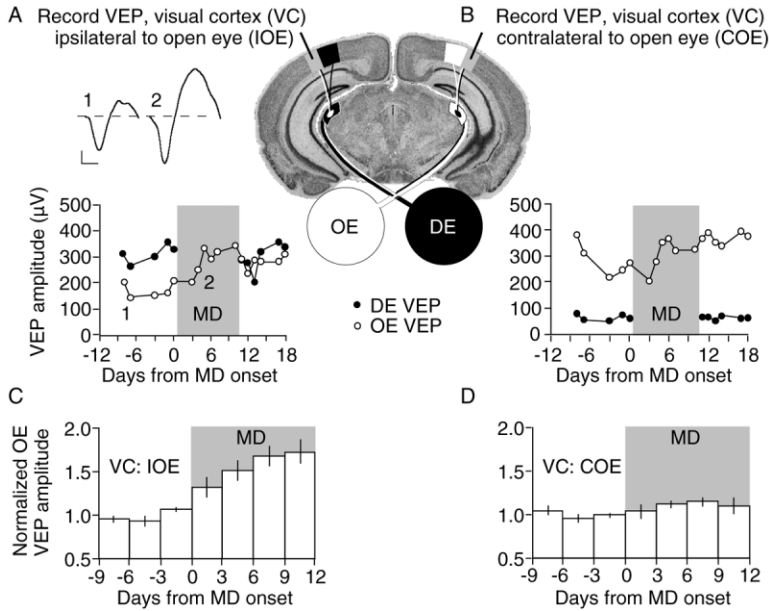In another group of adult animals (n = 4), VEP responses were followed for an additional period of binoc-

ular experience following MD (Figure 4). The ipsilateral-eye VEPs grew to 231% $\pm$ 18% of baseline after 12 days of contralateral-eye MD, and these were still significantly elevated after an additional 6 days of binocular experience (168% $\pm$ 17%; $p < 0.01$, Fisher's PLSD). In contrast, the VEPs evoked by stimulation of the deprived (contralateral) eye were not significantly affected by the period of MD (91% $\pm$ 16% of baseline) or subsequent binocular experience (105% $\pm$ 23%). These data show that the gradual enhancement of ipsilateral-eye VEPs during MD reflects a persistent modification.

To confirm that MD does induce synaptic depression in young mice, we examined the consequences of 3 day MD begun at P28 in chronically implanted animals (n = 5). Unlike adults, MD strongly depressed responses to stimulation of the deprived (contralateral) eye (24% $\pm$ 5% of baseline; $p < 0.01$; Fisher's PLSD). However, we observed no significant change in the ipsilateral-eye VEP during this brief period of MD. These findings show that comparable shifts in the C/I ratio in young and mature animals can be accounted for by different underlying mechanisms, and these can be dissociated. It should be noted, however, that longer periods of MD in young animals also eventually lead to enhanced responses to nondeprived ipsilateral-eye stimulation (our unpublished data).

Post hoc analysis of the adult MD experiments summarized in Figure 3C revealed that both the initial negative component and the later positive component of the ipsilateral-eye VEP waveform increased by a comparable amount following deprivation of the contralateral eye (by 184% $\pm$ 29% and 164% $\pm$ 13%, respectively, after 6–7 days of MD; n = 8). Because recordings were made at a depth of 400 μm, where the negative VEP is maximal, we can conclude that the short-latency current sink in layer IV/deep III is increased. This finding is consistent with the possibility that thalamocortical and/or short latency intracortical synaptic transmission is potentiated. Alternatively, however, it is possible that changes recorded in cortex after MD passively reflect modifications occurring subcortically. In order to distinguish among these alternatives, and to gain insight into the molecular mechanisms involved, we generated a line of mutants in which cortical, but not thalamic, NMDA receptor function is impaired.

Generation of Cortical NMDA Receptor Knockout Mice

A transgenic mouse strain, G35-3, was created in which the genetic promoter of a kainate-type glutamate receptor subunit (KA-1) directs Cre-recombinase expression. The spatial and temporal pattern of Cre/*loxP* recombination in the G35-3 Cre mouse line was examined by crossing it with a *lacZ* reporter mouse (Rosa26) and staining brain sections derived from the progeny with X-Gal. Cre/*loxP* recombination was first detectable at postnatal day 14. At 8 weeks of age, recombination had occurred in the majority of pyramidal cells in layer II–IV of the sensory neocortex, including area 17, and the hippocampus (Figure 5A). Double immunofluoresence staining of visual cortex with antibodies against β-galactosidase (a marker for Cre/*loxP* recombination) and glutamic acid decarboxylase (GAD)-67 or GABA (markers for inhibitory

A Record VEP, visual cortex (VC) ipsilateral to open eye (IOE)

B Record VEP, visual cortex (VC) contralateral to open eye (COE)

• DE VEP
○ OE VEP

C VC: IOE

D VC: COE

Figure 3. Chronic VEP Recordings in the Adult Mouse Reveal a Potentiation of VEP Amplitudes Ipsilateral to the Open Eye following MD

(A and B) Schematic of the mouse visual pathway and recording positions. VEP amplitudes recorded from a representative animal before, during (gray rectangle), and after MD are illustrated in the panels below (left, recording ipsilateral to the open eye [IOE]; right, recording contralateral to the open eye [COE]). Open symbols represent VEPs elicited by stimulation of the unmanipulated, open eye (OE). Filled symbols represent VEPs elicited through the deprived eye (DE), prior to or following deprivation. Note: VEP amplitudes recorded IOE increase dramatically between 3 and 5 days following the onset of MD (left panel). Traces are averages of 60 consecutive stimulus presentations taken at the times indicated by numbers. Scale bar, 50μV and 50 ms.

(C and D) Average VEP amplitudes recorded before and during a period of MD (left, recording IOE; right, recording COE). VEP amplitudes were normalized to the baseline period preceding the onset of MD.

interneurons) showed that recombination was restricted to excitatory cells. Recombination also occurred in frontal cortex, deep layers of parietal and occipital cortex, and amygdala, but at distinctly lower frequencies. No recombination was detected in the mesial neocortex, striatum, thalamus, or hindbrain. Recombination frequency did not change in older mice.

We then crossed the G35-3 line, (Cre$^{+/-}$), with homozygous floxed-NR1 mice (Tsien et al., 1996) to obtain doubly floxed-NR1 mutant mice (Cre$^{+/-}$, NR1$^{floxed/floxed}$). We further crossed this mutant animal with heterozygous NR1 null mutant mice (NR1$^{+/-}$) (Li et al., 1994) to obtain four types of mice: Cre$^{+/-}$, NR1$^{floxed/-}$; Cre$^{+/-}$, NR1$^{floxed/+}$; Cre$^{-/-}$, NR1$^{floxed/-}$; Cre$^{-/-}$, NR1$^{floxed/+}$. The first mouse genotype, Cre$^{+/-}$, NR1$^{floxed/-}$, constitutes a cortex-NR1 knockout, hereafter referred to as CxNR1KO mice. As a control animal, we used Cre$^{-/-}$, NR1$^{floxed/-}$ mice (hereafter referred to as control), in which cortical NMDA receptor function was previously shown to be normal (Iwasato et al., 1997).

CxNR1KO mice were viable and fertile, and exhibited no gross developmental abnormalities. In situ hybridization experiments indicated that the NR1 gene is still intact at P30 (data not shown). The delay in Cre/*loxP* recombination-dependent deletion of NR1 relative to the expression of the *lacZ* gene in the Rosa26 mouse has been documented previously (Nakazawa et al., 2002) and is likely due in part to differences in the susceptibility of the *loxP* substrates to the recombinase. However, we found that by P70, NR1 mRNA is ablated in about 50% of layer II–IV cells in the binocular region of mutant visual cortex (Figure 5B). Of the cells that continue to express NR1, a significant fraction (20% of all cortical neurons) are GABAergic interneurons. Therefore, we estimate that at least two thirds of layer II–IV pyramidal cells lack NMDA receptor function at 10 weeks of age. An NR1 ablation was not observed in the deep layers (V/VI) of the visual cortex nor in the thalamus.

To characterize NMDAR function in visual cortex of

wild-type, control, and CxNR1KO mice, we measured NMDAR-mediated currents from visually identified layer II/III pyramidal cells. NMDAR-mediated currents were pharmacologically isolated as previously described (Philpot et al., 2001). Cells were voltage-clamped at +40mV, and input-output curves were generated by recording NMDA EPSCs evoked by stimulation of layer IV at escalating intensities (see Experimental Procedures). Every layer II/III pyramidal cell recorded from C57BL6/J wild-type (n = 16) and control mice (n = 10) exhibited NMDAR-mediated currents (Figure 5C). In contrast, a large population of cells recorded from CxNR1KO mice failed to exhibit NMDAR-mediated currents. A 11 × 3 repeated measures mixed-effect ANOVA, with stimulation intensity as the 11 level between group

A Adult MD (contra eye)

■ Contra eye VEP
□ Ipsi eye VEP

B Young MD (contra eye)
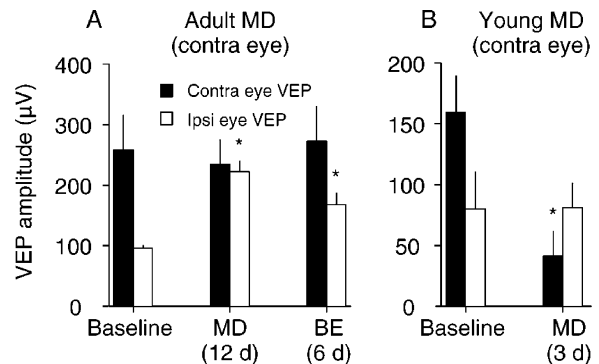
Figure 4. Effects of Adult MD are Persistent and Qualitatively Different from Juvenile MD

(A) Contralateral (filled bars) and ipsilateral (open bars) VEP amplitudes measured during a baseline period, following 12 days of MD, and again 6 days after restoring binocular experience (BE) in adult mice. Recordings were conducted in the hemisphere contralateral to the deprived eye for both (A) and (B).

(B) Contralateral (filled bars) and ipsilateral (open bars) VEP amplitudes measured during a baseline period and again after 3 days of MD initiated at P28.
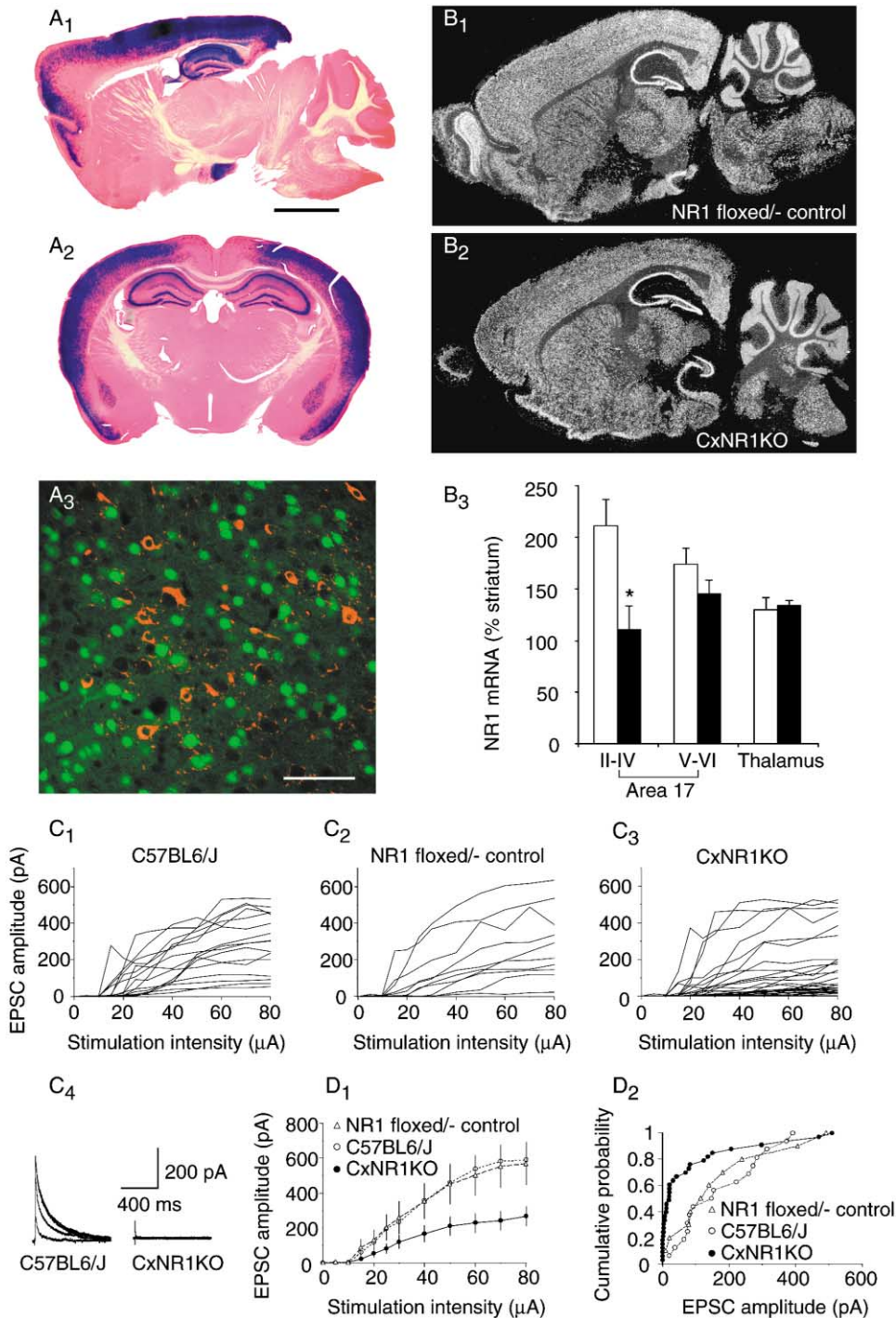
Figure 5. Distribution of Cre Recombination and Reduction of Neocortical Layer II/III NR1 mRNA and NMDA Receptor-Mediated EPSCs in the CxNR1KO Mice

(A) Parasagittal (A_1) and coronal (A_2) sections from the brains of a 10-week-old male G35-3/Rosa26 double-transgenic mouse stained with X-Gal and Nuclear Fast Red. Scale bar in (A_1), 3 mm, applies to (A_2), (B_1), and (B_2). (A_3) Cortical sections from the brain of a 10-week-old male G35-3/Rosa26 mouse subjected to double immunofluorescent staining with antibodies against β-galactosidase (green) and GAD-67 (red). Scale bar, 200 μm.

(B) Dark-field images of in situ hybridization performed on coronal sections taken from a 10-week-old male control (Cre$^{-/-}$; NR1$^{floxed/-}$) and his mutant littermate (Cre$^{+/-}$; NR1$^{floxed/-}$) using a ^{33}P-labeled NR1 cRNA probe. Scale bar, 2 mm. (B_3) Densitometric analysis of NR1 mRNA in area 17 layers II–IV, layer V/VI, and dorsal thalamus. Relative optical density was normalized for each section (eight sections from three animals for each genotype) to the signal level of the striatum. Open bar, control; filled bar, mutant; *p < 0.01.

(C_1–C_3) Pharmacologically isolated NMDA receptor-mediated EPSC amplitudes from individual layer II/III pyramidal cells plotted as a function of layer IV extracellular stimulation intensity. Input-output curves were generated in C57BL6/J wild-type (C_1), control (C_2), and CxNR1KO (C_3) mice.

(C_4) Representative EPSCs evoked by 20, 40, 60, and 80 μA in C57BL6/J and CxNR1KO mice. Stimulus artifacts have been clipped for clarity.

(D_1) Averaged input-output curves demonstrating attenuated NMDAR function in layer II/III pyramidal cells from CxNR1KO mice.

(D_2) Cumulative probability histogram of EPSC amplitudes evoked by 40 μA stimulation. Note that in CxNR1KO mice, there is a large population of cells that do not exhibit NMDA-mediated currents, but there is also a population of cells that exhibit normal currents.
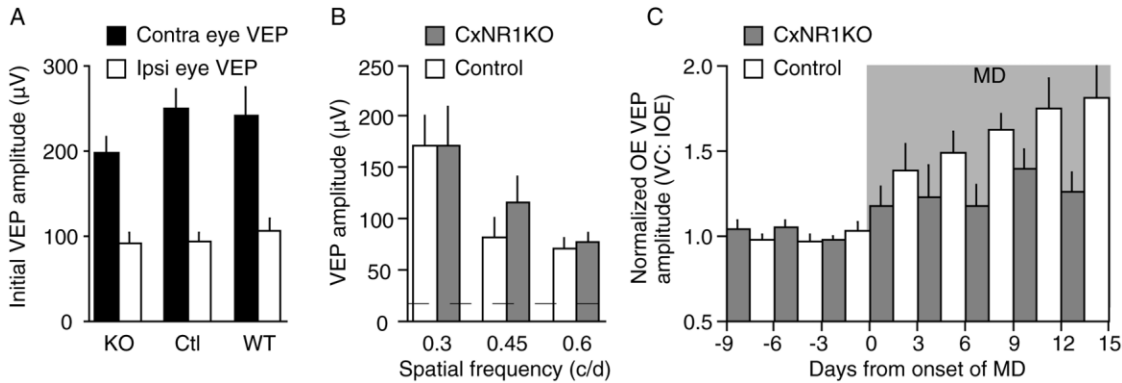
Figure 6. Potentiation of VEP Amplitudes following MD Is Absent in Adult Mice Lacking Functional NMDA Receptors in Visual Cortex

(A) Initial contralateral (filled bars) and ipsilateral (open bars) VEP amplitudes measured on day 1–2 of the baseline recording period. Data from the right and left visual cortices were pooled for each animal.

(B) VEPs evoked by gratings of various spatial frequencies (0.3, 0.45, and 0.6 cycles/degree) in control and CxNR1KO mice. The dashed line indicates the response to a grating of 0% contrast.

(C) VEPs evoked by pattern visual stimulation of the ipsilateral (nondeprived) eye in awake, head-restrained heterozygote (control, open bars) and NR1 knockout (CxNR1KO, hatched bars) mice prior to and during a period of MD (shaded rectangle).

effect and genotype as the 3 level effect, indicated a significant consequence of genotype [$F_{(2,560)} = 5.0$, $p < 0.02$] and stimulation intensity [$F_{(10,560)} = 71.6$, $p < 0.0001$] on EPSC amplitude, as well as a significant interaction between stimulation intensity and genotype [$F_{(20,560)} = 5.26$, $p < 0.0001$]. Post hoc analysis using the Bonferroni/Dunn tests revealed that NMDAR-mediated currents were significantly attenuated in cells from CxNR1KO as compared to C57BL6/J wild-type and floxed/− control mice ($p < 0.0001$; Figure 5D). This difference appears to arise because one population of cells in the CxNR1KO mice did not exhibit NMDAR-mediated currents, while another population of cells exhibited normal NMDAR-mediated currents, similar to those observed in C57BL6/J wild-type and floxed/− control mice (Figure 5D).

Adult Ocular Dominance Plasticity Is Cortical and Requires NMDA Receptors

Having established a deficit in cortical NMDAR function in the adult CxNR1KO mouse, we next tested whether enhancement of open-eye VEP responses following MD was altered in these animals. Chronic VEP recordings were performed as described previously, with experimenters blind to genotype. Initial VEP amplitudes evoked by contralateral- and ipsilateral-eye stimulation, and C/I ratios, were not significantly different in wild-type, control, and CxNR1KO mice (Figure 6A). VEP amplitudes were also comparable across a range of stimulus spatial frequencies (Figure 6B), suggesting that visual acuity was not impaired as a result of the postadolescent NR1 knockout. Nonetheless, the cortical response to MD clearly differed across genotypes. In control mice, VEP amplitude increases following MD were similar in magnitude and kinetics to those observed in wild-type mice (175% ± 18.2% of baseline days 9–11 post-MD, n = 9; Figure 6C). In contrast, MD had no significant effect in CxNR1KO mice [n = 8; repeated measures ANOVA; $F_{(7,49)} = 1.92$; $p > 0.08$]. VEP amplitudes recorded during the MD period in CxNR1KO and control mice were

significantly different; a two-factor repeated measures ANOVA revealed a significant effect of time by genotype [$F_{(7,105)} = 2.849$; $p < 0.01$].

Because Cre/loxP recombination and consequent NR1 knockout was delayed until after adolescence and restricted to the forebrain, the diminished effects of MD in these animals strongly suggests that enhancement of open-eye inputs is occurring at the level of the primary visual cortex. Moreover, like other forms of synaptic enhancement—including long-term potentiation (LTP) induced in the adult rodent visual cortex by thalamic stimulation (Heynen and Bear, 2001)—increases in open-eye VEP amplitude following MD require NMDA receptor activation. Thus, it appears that we have observed, in real time, a process of experience- and NMDAR-dependent LTP in the neocortex.

Discussion

Our data reveal a novel form of binocular competition in the adult visual cortex. Patterned activity in the ipsilateral eye drives mechanisms of synaptic enhancement when an inhibitory constraint imposed by activity in the dominant contralateral eye is removed. This cortical adaptation to loss of the dominant input is not immediate, but appears to require several days. These findings are consistent with the notion of metaplasticity—that the conditions required to induce synaptic plasticity depend on the history of cortical activity (Abraham and Bear, 1996). We propose that the overall reduction in cortical activity caused by depriving the contralateral eye lowers the "modification threshold" and enables visual experience to drive ipsilateral-eye enhancement (Bear, 1995; Kirkwood et al., 1996). In the other hemisphere, however, total cortical activity is hardly affected by deprivation of the ipsilateral eye, and therefore no modifications are observed. We note that binocular competition implemented by a sliding modification threshold is a key prediction of the BCM theory of synaptic plasticity (Bienenstock et al., 1982; Clothiaux et al., 1991).

Deprivation-enabled plasticity appears to be a universal property of adult neocortex. For example, silencing the principal input to a region of somatosensory cortex enables the progressive potentiation of initially weak inputs from other regions of the body surface. This effect has been observed in a wide range of species, including primates (Diamond et al., 1993; Fox, 2002; Merzenich et al., 1983; Rasmusson, 1982). Similarly, visual cortical neurons that are silenced by focal retinal lesions rapidly acquire new receptive fields in adult cats and monkeys (Dreher et al., 2001; Gilbert and Wiesel, 1992; Kaas et al., 1990). The mechanisms that account for these findings, while presently unknown, are likely to serve perceptual learning and information storage by the neocortex (Gilbert et al., 2001). Our data indicate that enhancement of the initially weak ipsilateral-eye input, enabled by deprivation of the dominant contralateral-eye input, is experience- and NMDAR dependent. It is interesting to note that one consequence of silencing the visual cortex is a gradual change in the properties and subunit composition of synaptic NMDARs, and this has been proposed to be a molecular basis for the sliding modification threshold (Philpot et al., 2001; Quinlan et al., 1999). The mouse model of adult ocular dominance plasticity described here offers a new opportunity to test this and other mechanistic hypotheses. It seems likely that any insights gained in the relatively undifferentiated visual cortex of mice will apply broadly to the understanding of synaptic plasticity in the neocortex of all mammals.

The classic studies of MD in kittens by Hubel and Wiesel (1970) led to the notion of a critical period for synaptic plasticity in visual cortex that ends around the onset of adolescence. While it has been well established in numerous species that modifications are most readily elicited by MD early in postnatal development, detailed analysis in cats and rats has shown that OD plasticity tapers slowly and can linger well beyond sexual maturity (Daw et al., 1992; Guire et al., 1999). Our data in mice support this conclusion; however, they also suggest that the qualities of OD plasticity vary significantly with age. While the delayed potentiation of the nondeprived ipsilateral-eye response continues to occur as late as P90 (the oldest age examined), the rapid depression of deprived-eye responses is greatly reduced or absent in mice older than P35. In this context it is interesting to note that in slices of mouse visual cortex, LTP can be elicited beyond P35, but NMDAR-dependent long-term depression (LTD) cannot (Kirkwood et al., 1997). Understanding the basis for the developmental decline in LTD, therefore, is likely to yield important insights into how deprivation-induced synaptic depression is regulated by age (Bear and Rittenhouse, 1999).

Our data demonstrate that an OD shift can occur in mice by depression of deprived-eye responses, enhancement of open-eye responses, or both, and the relative contributions of these mechanisms can vary with age and MD duration. This revelation may force a revision in how the effects of various mutations have been interpreted. For example, OD plasticity, as measured by changes in the C/I ratio, clearly can survive developmental downregulation of the mechanism of deprivation-induced synaptic depression. Thus, finding that OD plasticity still occurs in a mutant mouse that lacks this mechanism could lead to the misleading conclusion that it is unimportant for OD plasticity in wild-type animals. In addition, it now becomes imperative to ask if mutations that alter the course of the critical period do so by changing the quality or the quantity of synaptic plasticity. Although our findings suggest that OD plasticity in mice is more complicated than previously assumed, we are encouraged to believe that it may now be possible to perform a genetic dissection of the mechanisms of naturally occurring synaptic enhancement, depression, and metaplasticity in visual cortex in vivo.

Experimental Procedures

Acute VEP Recordings

Acute electrophysiological recordings were carried out in male C57Bl/6 mice (Charles River, Cambridge, MA) under urethane anesthesia (Sigma, 8 ml/kg). Anesthetic depth was monitored by testing reflexes and observing the frequency of bursting activity in local field potentials recorded in the visual cortex (typically 0.5–2 Hz) (Fox and Armstrong-James, 1986). Measurements of the C/I VEP ratios were obtained promptly (<1 hr) after induction of anesthesia to minimize variability due to changes in the depth of anesthesia. VEPs were recorded from the dural surface overlying area 17 with resin-coated tungsten microelectrodes (WPI, Sarasota, FL; 0.5 MΩ). Positioning of electrodes within the binocular visual cortex was verified in two ways. For each recording site, the region of the visual field yielding maximal VEP amplitudes was established by recording a series of responses to stimuli windowed to a vertical or horizontal stripe occupying 10° × 110° of the visual field and presented at several visual field azimuths and elevations. Electrode position was then adjusted such that VEP amplitudes were maximal for a vertical window centered 0°–20° from the vertical meridian, thus well within the binocular visual field of the mouse. In addition, after many experiments electrolytic lesions (10–20 μA, 5 s) were made to mark recording sites, and lesions were located within A17 using Nissl-stained sections, according to established cytoarchitectonic criteria (Caviness, 1975). Electrical signals were amplified (1000×), filtered (0.1 Hz and 3.0 kHz), digitized at 20 kHz, and averaged (>100 events per block) in synchrony with the stimulus contrast reversal using an IBM compatible computer running custom software written in LabView (National Instruments, Austin, TX) and provided courtesy of the lab of Professor L. Maffei (Pisa, Italy). Transient VEPs in response to abrupt contrast reversal (1 Hz) were analyzed in the time domain by measuring the amplitude and latency of the positive peak of the major response component. VEPs in response to a stimulus of 0% contrast were also frequently recorded as an estimate of stimulus-independent cortical activity.

CSD Analysis

CSD analysis was performed as described by Heynen and Bear (2001).

Chronic Surgical Procedures and VEP Recording

Mice were anesthetized with 50 mg/kg ketamine and 10 mg/kg xylazine i.p., and a local anesthetic of 1% lidocaine hydrochloride was injected over the scalp. For purposes of head fixation, a post was fixed to the skull just anterior to bregma using cyanoacrylate and a further application of dental cement. Two small (<0.5 mm) burr holes were made in the skull overlying the binocular visual cortex, and tungsten microelectrodes (FHC, Bowdoinham, ME) were inserted 400 μm below the cortical surface. Electrodes were secured in place using cyanoacrylate, and the entire exposure was covered with dental cement. Animals were monitored postoperatively for signs of infection or discomfort and allowed at least 24–48 hr recovery before the first recording session.

VEP recordings were conducted in awake, head-restrained mice. Following the recovery period, animals were handled and habituated to head restraint. Once habituated, animals sat quietly with minimal movement for the duration of a recording session (approximately 1 hr). Pattern visual stimuli were presented alternately to right and the left eyes (60–100 stimuli/block). Each stimulus condition was repeated at least six times over the course of a recording session.

Although VEP amplitudes were routinely quantified by measuring the peak-peak response amplitude, the results of our experiments were identical if only the peak negativity was measured. Statistical analyses were performed using StatView 5.0.1 (Abacus Concepts, Berkeley, CA). Potential group differences in contra/ipsi VEP amplitudes following monocular deprivation were evaluated by factorial and repeated measures analyses of variance (ANOVA), and relevant post hoc comparisons were made using Fisher's protected least square difference (PLSD) analysis. In all cases, significance was set at $p < 0.05$.

Visual Stimuli

Visual stimuli consisted of full-field sine wave gratings of 100% contrast and 0.5 cycles/degree generated by a VSG2/2 card (Cambridge Research System, Cheshire, UK) and presented on a computer monitor suitably linearized by γ correction. The display was positioned 20 cm in front of the mouse and centered on the midline, thereby occupying $110° \times 82.5°$ of the visual field. Mean luminance, determined by a photodiode placed in front of the computer screen, was 27 cd/m^2.

Monocular Deprivation

Monocular deprivation was performed by eyelid suture. Mice were anesthetized by inhalation of isoflurane (IsoFlo 2%–3%) and placed under a surgical microscope. Lid margins were trimmed and the antibiotic (Vetropolycin, Pharmaderm) was applied to the eye. Three to five mattress stitches were placed using 7-0 silk, opposing the full extent of the trimmed lids. Animals were recovered by breathing room air and were monitored daily to be sure that the sutured eye remained shut and uninfected. Animals whose eyelids did not fully seal shut were excluded from further experiments. At the end of the deprivation period, mice were reanesthetized, stitches were removed, and lid margins were separated. Eyes were then flushed with sterile saline and checked for clarity under a microscope. Mice with corneal opacities or signs of infection were excluded from further study.

Voltage-Clamp Recordings from Visual Cortex Slices

Slices were prepared, and pharmacologically isolated NMDA receptor-mediated EPSCs were recorded, as described by Philpot et al. (2001). Input-output curves were generated by recording EPSC amplitude in layer II–III pyramids evoked by stimulation of layer 4 with 5, 10, 15, 20, 25, 30, 40, 50, 60, 70, or 80 μA. Two EPSCs were averaged at each stimulation intensity. Note that at higher stimulation intensities (≥ 40 μA), a small (<10 pA) non-NMDA component was sometimes observed that was resistant to both the NMDAR antagonist AP5 (Sigma, 100 μM) and GABA$_B$ receptor antagonist CGP35348 (Tocris, 100 μM) (data not shown).

Generation of Cortex-NR1 Knockout Mice

We obtained a Cre-recombinase transgenic strain by coinjecting Cre-cDNA and BAC1 containing a part of the genomic sequence of mouse KA-1, one of the kainate receptor subunits, into fertilized B6 mouse eggs as previously described (Nakazawa et al., 2002). The line referred to as G35-3 was crossed with the Rosa26 reporter line (Soriano, 1999) to visualize the distribution of Cre/loxP recombination. In order to generate cortex-NR1 knockout mice, the line was first crossed with the "floxed" NMDA receptor subunit-1 (fNR1) mouse line (Tsien et al., 1996) and subsequently backcrossed to B6 more than ten times. Doubly floxed-NR1 mutant mice (Cre$^{+/-}$, NR1$^{floxed/floxed}$) were further crossed with heterozygous NR1 null mutant mice (NR1$^{+/-}$) (Li et al., 1994) to yield CxNR1KO and control mice, as described in the text. All procedures relating to animal care and treatment conformed to institutional and NIH guidelines. Immunocytochemistry and in situ hybridization experiments were performed as described previously (Nakazawa et al., 2002). For quantification of NR1 mRNA levels, eight sections of three control or mutant mice were used to measure relative optical densities of area 17, dorsal thalamus, and striatum using Scion Image software (version β 4.0.2).

References

Abraham, W., and Bear, M. (1996). Metaplasticity: the plasticity of synaptic plasticity. Trends Neurosci. *19*, 126–130.

Aizenman, C., Kirkwood, A., and Bear, M. (1996). Current source density analysis of evoked responses in visual cortex in vitro: implications for the regulation of long-term potentiation. Cereb. Cortex *6*, 751–758.

Bear, M. (1995). Mechanism for a sliding synaptic modification threshold. Neuron *15*, 1–4.

Bear, M.F., and Rittenhouse, C.D. (1999). Molecular basis for induction of ocular dominance plasticity. J. Neurobiol. *41*, 83–91.

Bienenstock, E.L., Cooper, L.N., and Munro, P.W. (1982). Theory for the development of neuron selectivity: orientation specificity and binocular interaction in visual cortex. J. Neurosci. *2*, 32–48.

Caviness, V.S., Jr. (1975). Architectonic map of neocortex of the normal mouse. J. Comp. Neurol. *164*, 247–263.

Clothiaux, E.E., Bear, M.F., and Cooper, L.N. (1991). Synaptic plasticity in visual cortex: comparison of theory with experiment. J. Neurophysiol. *66*, 1785–1804.

Daw, N.W., Fox, K., Sato, H., and Czepita, D. (1992). Critical period for monocular deprivation in the cat visual cortex. J. Neurophysiol. *67*, 197–202.

Diamond, M.E., Armstrong-James, M., and Ebner, F.F. (1993). Experience-dependent plasticity in adult rat barrel cortex. Proc. Natl. Acad. Sci. USA *90*, 2082–2086.

Drager, U.C. (1978). Observations on monocular deprivation in mice. J. Neurophysiol. *41*, 28–42.

Dreher, B., Burke, W., and Calford, M.B. (2001). Cortical plasticity revealed by circumscribed retinal lesions or artificial scotomas. Prog. Brain Res. *134*, 217–246.

Fagiolini, M., and Hensch, T.K. (2000). Inhibitory threshold for critical-period activation in primary visual cortex. Nature *404*, 183–186.

Fox, K. (2002). Anatomical pathways and molecular mechanisms for plasticity in the barrel cortex. Neuroscience *111*, 799–814.

Fox, K., and Armstrong-James, M. (1986). The role of the anterior intralaminar nuclei and N-methyl-D-aspartate receptors in the generation of spontaneous bursts in rat neocortical neurones. Exp. Brain Res. *63*, 505–518.

Gilbert, C.D., and Wiesel, T.E. (1992). Receptive field dynamics in adult primary visual cortex. Nature *356*, 150–152.

Gilbert, C.D., Sigman, M., and Crist, R.E. (2001). The neural basis of perceptual learning. Neuron *31*, 681–697.

Gordon, J.A. (1997). Cellular mechanisms of visual cortical plasticity: a game of cat and mouse. Learn. Mem. *4*, 245–261.

Gordon, J.A., and Stryker, M.P. (1996). Experience-dependent plasticity of binocular responses in the primary visual cortex of the mouse. J. Neurosci. *16*, 3274–3286.

Guire, E.S., Lickey, M.E., and Gordon, B. (1999). Critical period for the monocular deprivation effect in rats: assessment with sweep visually evoked potentials. J. Neurophysiol. *81*, 121–128.

Hanover, J.L., Huang, Z.J., Tonegawa, S., and Stryker, M.P. (1999). Brain-derived neurotrophic factor overexpression induces precocious critical period in mouse visual cortex. J. Neurosci. *19*, RC40.

Hensch, T.K., Fagiolini, M., Mataga, N., Stryker, M.P., Baekkeskov, S., and Kash, S.F. (1998). Local GABA circuit control of experience-

dependent plasticity in developing visual cortex. Science *282*, 1504–1508.

Heynen, A.J., and Bear, M.F. (2001). Long-term potentiation of thalamocortical transmission in the adult visual cortex in vivo. J. Neurosci. *21*, 9801–9813.

Heynen, A.J., Yoon, B.-J., Liu, C.-H., Chung, L.J., Huganir, R.L., and Bear, M.F. (2003). Molecular mechanism for loss of visual responsiveness in visual cortex following early monocular deprivation. Nat. Neurosci., in press.

Huang, Z.J., Kirkwood, A., Pizzorusso, T., Porciatti, V., Morales, B., Bear, M.F., Maffei, L., and Tonegawa, S. (1999). BDNF regulates the maturation of inhibition and the critical period of plasticity in mouse visual cortex. Cell *98*, 739–755.

Hubel, D.H., and Wiesel, T.N. (1970). The period of susceptibility to the physiological effects of unilateral eye closure in kittens. J. Physiol. *206*, 419–436.

Iwasato, T., Erzurumlu, R.S., Huerta, P., Chen, D.F., Sasaoka, T., Ulupinar, E., and Tonegawa, S. (1997). NMDA receptor-dependent refinement of somatotopic maps. Neuron *19*, 1201–1210.

Kaas, J.H., Krubitzer, L.A., Chino, Y.M., Langston, A.L., Polley, E.H., and Blair, N. (1990). Reorganization of retinotopic cortical maps in adult mammals after lesions of the retina. Science *249*, 229–231.

Kirkwood, A., Rioult, M.G., and Bear, M.F. (1996). Experience-dependent modification of synaptic plasticity in visual cortex. Nature *381*, 526–528.

Kirkwood, A., Silva, A., and Bear, M.F. (1997). Age-dependent decrease of synaptic plasticity in the neocortex of αCaMKII mutant mice. Proc. Natl. Acad. Sci. USA *94*, 3380–3383.

Kossut, M., and Singer, W. (1991). The effect of short periods of monocular deprivation on excitatory transmission in the striate cortex of kittens: a current source density analysis. Exp. Brain Res. *85*, 519–527.

Li, Y., Erzurumlu, R.S., Chen, C., Jhaveri, S., and Tonegawa, S. (1994). Whisker-related neuronal patterns fail to develop in the trigeminal brainstem nuclei of NMDAR1 knockout mice. Cell *76*, 427–437.

Merzenich, M.M., Kaas, J.H., Wall, J.T., Nelson, R.J., Sur, M., and Fellerman, D. (1983). Topographic reorganization of somatosensory cortical areas 3b and 1 in adult monkeys following restricted deafferentation. Neuroscience *8*, 33–55.

Mioche, L., and Singer, W. (1989). Chronic recordings from single sites of kitten striate cortex during experience-dependent modifications of receptive-field properties. J. Neurophysiol. *62*, 185–197.

Mitzdorf, U. (1985). Current source-density method and application in cat cerebral cortex: investigation of evoked potentials and EEG phenomena. Physiol. Rev. *65*, 37–100.

Mitzdorf, U., and Singer, W. (1980). Monocular activation of visual cortex in normal and monocularly deprived cats: an analysis of evoked potentials. J. Physiol. *304*, 203–220.

Nakazawa, K., Quirk, M.C., Chitwood, R.A., Watanabe, M., Yeckel, M.F., Sun, L.D., Kato, A., Carr, C.A., Johnston, D., Wilson, M.A., and Tonegawa, S. (2002). Requirement for hippocampal CA3 NMDA receptors in associative memory recall. Science *297*, 211–218.

Philpot, B.D., Sekhar, A.K., Shouval, H.Z., and Bear, M.F. (2001). Visual experience and deprivation bidirectionally modify the composition and function of NMDA receptors in visual cortex. Neuron *29*, 157–169.

Porciatti, V., Pizzorusso, T., and Maffei, L. (1999). The visual physiology of the wild type mouse determined with pattern VEPs. Vision Res. *39*, 3071–3081.

Quinlan, E.M., Olstein, D.H., and Bear, M.F. (1999). Bidirectional, experience-dependent regulation of NMDA subunit composition in rat visual cortex during postnatal development. Proc. Natl. Acad. Sci. USA *96*, 12876–12880.

Rasmusson, D.D. (1982). Reorganization of raccoon somatosensory cortex following removal of the fifth digit. J. Comp. Neurol. *205*, 313–326.

Schroeder, C.E., Tenke, C.E., Givre, S.J., Arezzo, J.C., and Vaughan,

H.G., Jr. (1991). Striate cortical contribution to the surface-recorded pattern-reversal VEP in the alert monkey. Vision Res. *31*, 1143–1157.

Soriano, P. (1999). Generalized lacZ expression with the ROSA26 Cre reporter strain. Nat. Genet. *21*, 70–71.

Tsien, J.Z., Huerta, P.T., and Tonegawa, S. (1996). The essential role of hippocampal CA1 NMDA receptor-dependent synaptic plasticity in spatial memory. Cell *87*, 1327–1338.

Wiesel, T.N., and Hubel, D.H. (1963). Single cell responses in striate cortex of kittens deprived of vision in one eye. J. Neurophysiol. *26*, 1003–1017.